ISPRS Journal of Photogrammetry & Remote Sensing, 55(2): 94-104, 2000.

Design and Implementation of a Computational Processing System for Off-Line Digital Close-Range Photogrammetry

Clive S. Fraser [*], Kenneth L. Edmundson
Department of Geomatics
University of Melbourne
Parkville Vic 3052 Australia

Abstract

Through the adoption of recent innovations in automation in vision metrology, it can be demonstrated that rigorous, yet user-friendly digital photogrammetric processes of calibration and orientation/triangulation can be incorporated into a computational scheme which is on the one hand capable of meeting the demands of high metric quality, while on the other offering the facilities necessary to support wider application by non-specialist users. The software system *Australis*, developed for image mensuration and restitution of off-line close-range photogrammetric networks, is featured to illustrate these processes and procedures. By describing the structure and components of *Australis*, the authors aim to demonstrate that many processes which have on occasion been viewed to be the exclusive province of automated, high-precision vision metrology are indeed suited to more general application across a broad range of fields which involve 3D object recording via imagery.

Keywords: measurement automation; vision metrology; close-range photogrammetry; software systems; calibration; orientation

1. Introduction

It could well be argued that over the past half decade, broader adoption by non-specialist users of the technology of digital close-range photogrammetry has concentrated in two application domains (e.g. Fraser, 1998). The first is the use of highly automated off-line and on-line vision metrology systems for industrial measurement, whereas the second is in areas employing low-accuracy, low-cost systems which provide the capability of 3D model building. In the case of industrial vision metrology systems (e.g. Brown and Dold, 1995; Beyer, 1995; Ganci and Handley, 1998), successful commercial exploitation has come about through the development of specialised hardware components such as intelligent cameras, coded targets, measurement probes and exterior orientation (EO) devices. Also, the development of highly robust and automated photogrammetric orientation and calibration processes has contributed significantly. Systems designed more for general-purpose 3D modelling, such as Photomodeler (Eos Systems Inc., 2000) and ShapeCapture (ShapeQuest Inc., 2000), are often built on the same photogrammetric foundations, though they may in instances sacrifice the rigor of algorithms and procedures, and therefore accuracy potential, in order to exhibit a high degree of flexibility and ease-of-use. An example might be compromises in image mensuration precision where feature points are recorded by 'point-and-click' to the nearest pixel, rather than to the 0.02-0.04 pixel precision achieved in the measurement of special-purpose targets in vision metrology. Developments in digital close-range photogrammetry have by no means been restricted to these two general system categories, though it is true that the most significant commercial exploitation has occurred in automated industrial measurement and 3D model building using imagery from general-purpose digital frame cameras.

Commercial success generally provides an impetus to further development, and it is not too surprising therefore that many in the photogrammetric community are focussing upon further innovations in high-precision sensors and the associated sensor calibration and orientation/ triangulation procedures. As has been pointed out by Foerstner and Guelch (1999), however, the priorities of other users, such

[*] Corresponding author. E-mail: c.fraser@unimelb.edu.au (C. S. Fraser).

as the computer vision community, are focussed more upon both automation and a comprehensive exploitation of scene knowledge. Regrettably, accompanying a recognition of these divergent priorities is often the view that the two endeavours are to an extent incompatible. Thus, there is a school of thought that discounts advances in vision metrology in regard to their usefulness for more general-purpose automated sensor calibration and orientation. For example, the provision of targeting of any form might be regarded as an unacceptable operational constraint, even though the necessary target field might comprise just half a dozen points in the form of a simple EO device. We also hear the lament that sensor self-calibration is too specialised for broader, low accuracy applications of digital photogrammetry, and indeed constitutes an art. Yet a better focus of attention might be to ascertain whether a comprehensive sensor calibration is even necessary for the application being considered. Is there really a need to unnecessarily complicate an automatic sensor orientation of only modest metric quality given that for such a level of accuracy a reduced calibration model, which is often very stable over time, might suffice? The necessary calibration, for which there are established fully automatic procedures, could be carried out as a separate operation using some of the very aids that are seen to be a hindrance to general-purpose 3D scene reconstruction (e.g. the use of targets, or EO devices).

The comments above set the scene for the present paper, the basic aim of which is to demonstrate that rigorous, yet user-friendly digital photogrammetric processes of calibration and orientation/ triangulation can be incorporated into a computational process which is on the one hand capable of meeting the demands of high metric quality, while on the other offering the facilities necessary to support a broader field of applications by non-specialist users of digital photogrammetry. In order to illustrate these processes and procedures, the software package *Australis* is featured. This system for off-line close-range digital photogrammetry has been developed primarily as both an educational tool, and as a computational platform to support applied research. It also serves, however, as a very practical tool for routine semi-automated sensor calibration and orientation/triangulation. By describing salient features of *Australis*, the authors aim at illustrating that many processes, which have on occasion been viewed to be the exclusive province of high-precision vision metrology, are indeed suited to more general application.

2. Process structure

The various components of the computation processes to be discussed are perhaps best illustrated through reference to the basic user-interface structure of *Australis*, which comprises three main elements: a Project View, an Image View and a Graphics View, as indicated in Figs. 1, 2 and 3.

2.1. The Project View

The Project View embodies project management aspects as well as the essential elements of the photogrammetric measurement process, namely the camera(s) employed, the imagery to be measured, and the optional provision of supporting data such as object space information comprising scale constraints, and object point coordinates for datum assignment or network orientation.

Shown by **A** in Fig. 1 are a number of camera icons, each indicating a separate camera contained within a database of commonly used sensors. The cameras can be digital or metric analogue, though in the latter case it is assumed that the imagery is scanned and fiducial mark calibration is available. Associated with each camera is a calibration file (**B** in Fig. 1), which provides essential data regarding sensor and pixel size, along with values for the standard 10-term, ‘physical’ calibration model comprising interior orientation elements (x_o, y_o, c), lens distortion coefficients (K_1, K_2, K_3, P_1 and P_2) and terms for differential scaling and non-orthogonality between the x- and y-axes (b_1, b_2) (e.g. Fraser, 1997). The selection of the parameters to be employed in a sensor calibration can be made by the user, or an appropriate default set can be readily adopted. At the outset, it is generally necessary only to have a coarse estimate of the principal distance, c.

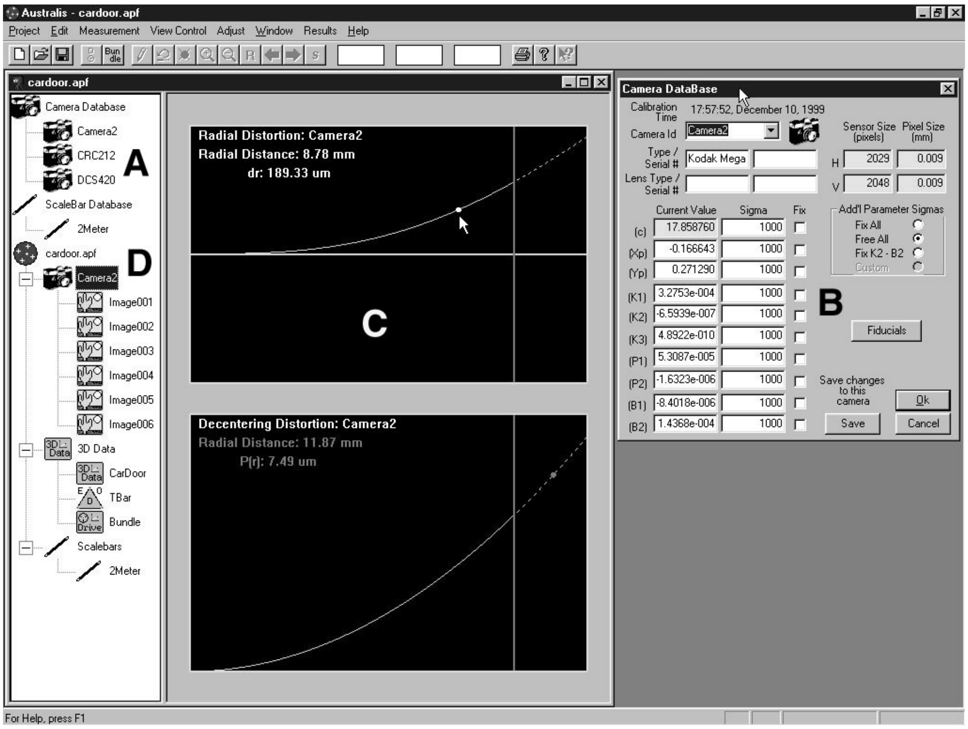

Fig.1. The Project View.

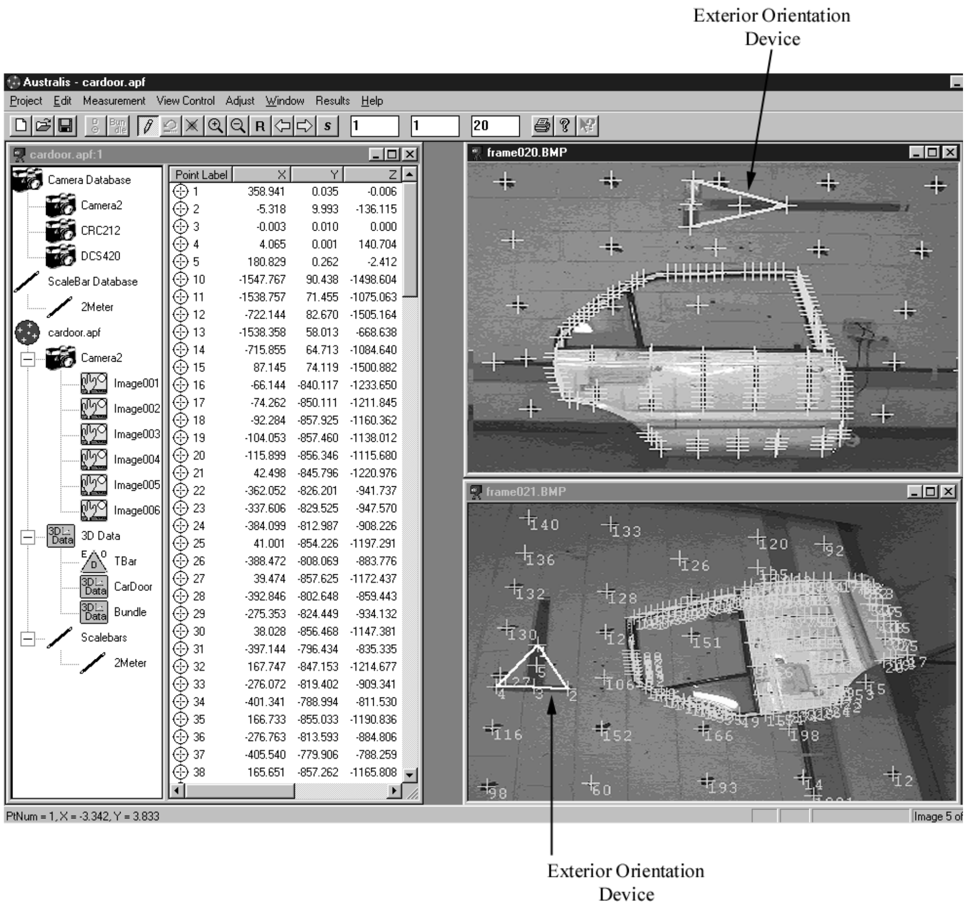

Fig. 2. The Image View.

To aid in an evaluation of the lens distortion, the radial and decentering distortion profiles can be displayed, as indicated by ‘C’ in Fig. 1. An important feature here is the vertical line beyond which the profile is dashed. This indicates the maximum radial distance used in any of the images forming the network for camera self-calibration. Thus, the dashed line represents the portion of the two profiles which is extrapolated (since the maximum possible radial distance can be larger than the maximum radial distance actually used in self-calibration), and which might well be avoided in subsequent triangulation using the estimated lens distortion parameters.

To initiate a photogrammetric network formation, a camera (or cameras) must be assigned to the project, which is effected simply by dragging and dropping the appropriate camera icon(s) into the project area (**D** in Fig. 1). The images are then selected for association with the appropriate camera. There is no set limit to the number of cameras or images and several hundred images can be accommodated. The practical limit to image file size is currently about 25 MB. The reason that many sensors can be handled is to support multi-ray triangulation from networks of multiple cameras with fixed exterior orientation, as encountered in photogrammetric systems for 3D motion analysis applications such as human movement studies, or in cases involving multi-sensor, multi-epoch measurement of dynamic events or structural deformation.

With only the sensor information and associated images at hand, one has the means to perform the 3D object reconstruction at an arbitrary orientation and scale, and possibly also the means to undertake a sensor calibration. However, without supplementary object space information, full automation of the restitution process is precluded. There is thus a need to associate object space coordinate information with the project. This may be in the form of preliminary XYZ coordinates for object points to support ‘resection driveback’. Or, it may comprise the coordinates of an EO device, which is placed in the field of view of the camera for either all or a subset of the camera stations in order to support initial fully automated exterior orientation. An EO device is simply an automatically recognisable cluster of targets, usually 4 to 6, which have known XYZ coordinates in a local reference system. The targets are in a geometric arrangement which is conducive to automatic recognition and also to closed-form determination of spatial resection. A robust closed-form resection, providing sufficiently accurate initial sensor EO values, can be achieved even with a relatively small EO device, so long as the target coordinates of the device are reasonably precise. For example, an EO device with a maximum target separation of 20 cm can give a sufficiently accurate initial resection for distances of up to 10 m for a large-area CCD camera with 20mm lens. An example EO device can be seen in Fig. 2 (see arrow). Control point information for datum assignment can also be input, as can scale information in the form of point-to-point distances. One feature of *Australis* is the ability to use scale data, either rigorously in the bundle adjustment as an observed distance of known *a priori* precision, as is needed to support self-calibration in multi-camera networks through the use of ‘wands’ (e.g. Maas, 1998), or as a means to simply scale the final object space coordinates after the network adjustment.

With these elements in place, along with the option to set various program preferences, the next stage of the photogrammetric process is embarked upon. This comprises the image mensuration and preliminary orientation phase.

2.2. The Image View

A prerequisite to fully automated image mensuration is an approximate knowledge of sensor EO. Irrespective of whether image coordinate measurement is via feature-based matching of interest points, least-squares template matching or centroiding of elliptical targets, the effectiveness of necessary solutions of both the image point correspondence problem and the process of resection driveback are influenced by the quality of the initial EO. In recognition of this, EO devices have recently become popular and they can prove very beneficial and practical for a wide range of applications, irrespective of whether the 3D scene to be reconstructed is targeted or otherwise.

Within the *Australis* image mensuration stage, most of the automated processes are contingent upon a preliminary EO, whether it be via an EO device or a more traditional resection approach based on measured 'control' points. Prior to EO, however, there is one process that can be carried out to support automatic measurement of well-defined image points such as retro-reflective targets. This is an operation which could be termed 'whole-image scanning', whereby a preliminary search is made for all valid targets within an image. Following recognition, extraction and validation, special geometric arrangement of targets forming either number codes or an EO device can be identified. Fraser and Shao (1997) have reported on a computational strategy for whole-image scanning, which is suitable to object scenes comprising target arrays and this constitutes a first automated image measurement step in *Australis*.

As an example, the upper image window shown in Fig. 2 displays the labels of an EO device, along with unlabelled centroids of object target points. This result is achieved via the whole-image scan. The lower image window in Fig. 2 shows a similar situation which is distinguished by the fact that the targets are labelled. Although this labelling is most often achieved via resection driveback, a viable alternative in situations where there is no preliminary object space coordinate information, but there is an EO device or known EO, is to achieve a point matching and labelling via a solution to the image point correspondence problem. Any of a number of methods can be employed for homologous image point determination, most of which employ epipolar line or plane geometry (e.g. Maas, 1992; Ariyawansa and Clarke 1997; Furnee et al., 1997). A most practical solution is to integrate the two approaches: a minimal set of images is employed to effect a solution to the image point correspondence problem for all object feature points, and then resection driveback is employed to measure image coordinates for the remaining images forming the network. For complex networks this process may need to be iteratively carried out, though for more straightforward network configurations it can be a fully automatic procedure (e.g. Ganci and Handley, 1998). The concept of coded targets can also be beneficial at this stage.

Referring back to the example of *Australis*, whole-image scanning can be effected for a single image or for all images. Images are automatically 'enabled' and 'disabled' depending on the success of the image point measurement process, and in the case of resection driveback, image coordinate residuals can be displayed (see right image in Fig. 3), as a means to support quality assessment.

A further feature supporting automation in image measurement in *Australis* is the ability to handle multi-epoch data sets, where the imagery has typically been acquired by multi-camera network configurations with nominally stable EO. In this instance, it is very common for an image at a given epoch to be very similar to that recorded with the same camera at the previous epoch, even though small deformations (object point movements) may have occurred. Here, information from the previous image can be employed to 'drive' the measurement of each successive image. In this operation, it may also be useful to automatically assign new point labels for any object points subject to deformation. This process is exemplified by a recently conducted deformation survey of a steel beam as it cooled from close to 1000°C to room temperature. Close to 80 epochs of data were collected over several hours in a network of three 2/3″ CCD cameras, where the object array consisted of 10 points on the beam (subject to movement) and 20 points away from the beam (assumed to be stable). The 'repeat measurement' feature in *Australis* allowed all images to be automatically measured in such a way that points subject to movement were given new labels at each epoch, whereas stable points kept the same labels. Once the 240 or so images had been measured, it was a simple matter, again within *Australis*, to carry out bundle adjustments incorporating anywhere from 3 images (single epoch) to 30 images (10 epochs) or 240 images (all epochs). With the required point re-labelling for deformation monitoring points, a sample interim bundle adjustment of 195 images included 660 object points and took 2.5 minutes per iteration to process.

As a final word on the image view, *Australis* also supports the measurements of 'plumb-lines' for plumb-line calibration of cameras, as well as features such as lines of targets, etc. It also supports measurement of non-signalised points, albeit only manually and therefore accurate to 0.3-0.5 pixels. The program does not presently support automated feature point extraction through interest operators, since attempts to fully automate the subsequent image matching have proven in many cases to be quite problematic for highly convergent networks and those in which there is a considerable range of perspective disparity. Whilst it is acknowledged that scene knowledge can contribute to making this problem more tractable, an enhancement to the level of automation by keeping the problem domain as straightforward as possible has been preferred in the development of *Australis*. This also assists ease-of-use by non-specialists.

2.3. The Graphics View

The third principal stage of the computational process incorporated in *Australis* comprises essentially three elements, which are grouped for ease of description under the term Graphics View. Upon leaving Image View, it is assumed that either all or a sufficient number of the images forming the network have been measured and have had their EO determined, albeit generally to only moderate accuracy. The network is thus ready for subsequent bundle adjustment or, alternatively, straightforward spatial intersection. Following 3D reconstruction, tools for network analysis can be employed. These comprise straightforward OPEN GL graphics displays of the network geometry for visual interpretation (e.g. Fig. 3), as well as an integrated process for 3D coordinate transformation and routines to compute best-fitting planes and lines, to name but two of the best-fit options.

The first stage of the process under the Graphics View is invariably a bundle adjustment, whether for sensor self-calibration, or to perform a precise multi-image triangulation for object point determination. In the interests of automation and ease-of-use, invoking the bundle adjustment should be possible with a minimum of operator intervention. In the case of *Australis*, one need only click on 'GO' in the dialog box indicated in Fig. 4 and a 'green light' or 'red light' will result.

The 'one-button' operation is feasible for two reasons. Firstly, all necessary image-related information to support a successful bundle adjustment is put in place during the processing associated with Image View, including the preliminary checking of observation data for blunders. Secondly, the options related to the bundle adjustment, such as observational error detection and the assignment of a datum for the object space coordinate system, default to choices supporting optimal automation and minimal user interaction. So, for example, automatic error detection is used, as is free-network adjustment via inner constraints. While the latter is useful in that it yields a minimal mean variance of object point coordinates for minimally constrained networks (e.g. Fraser, 1996; Mason 1994), it also requires no user-input of XYZ coordinate 'control'. The option of using object space control and of manually setting various preferences is available, and these options assume importance from an educational standpoint. Use of control points, however, does little to enhance user-friendliness of digital photogrammetry for non-specialists.

One of the noteworthy features of the *Australis* bundle adjustment is that it supports both forward and reverse fold-in within the normal equation reduction process. The forward fold-in describes the traditional process by which parameters relating to object point coordinates are eliminated from the normal equations, thus leaving a reduced system comprising only EO and camera calibration parameters (e.g. Brown, 1976). This algorithm is particularly beneficial when the number of object points greatly exceeds the number of images. In automated digital close-range photogrammetry, however, it is not unusual for the number of images to equal or exceed the number of object points. In this instance, it is both faster and arguably more straightforward to employ a reverse fold-in, whereby the camera station parameters are eliminated and the object point coordinate correction terms and self-calibration parameters are retained.

An analysis of the computational implications of forward and reverse fold-in is provided in Edmundson and Fraser (1998). Here, it is sufficient to give indicative figures for the performance of *Australis*. One iteration of a 50-image, 50-point self-calibrating bundle adjustment takes 58 seconds

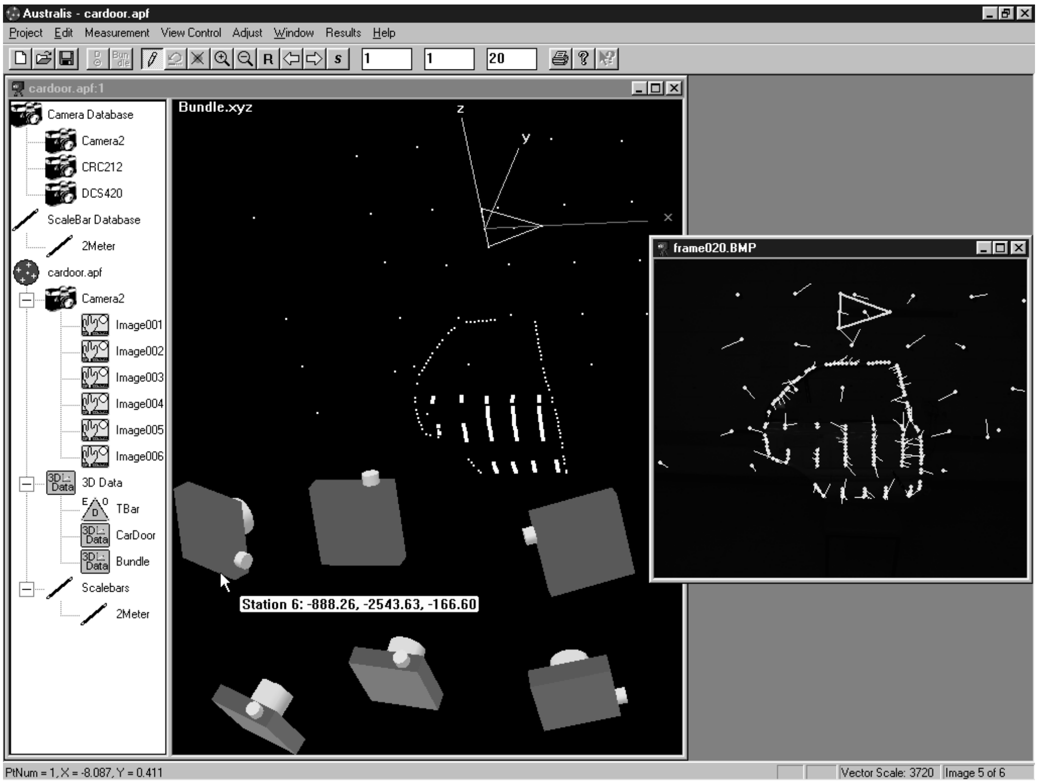

Fig. 3. The Graphics View.

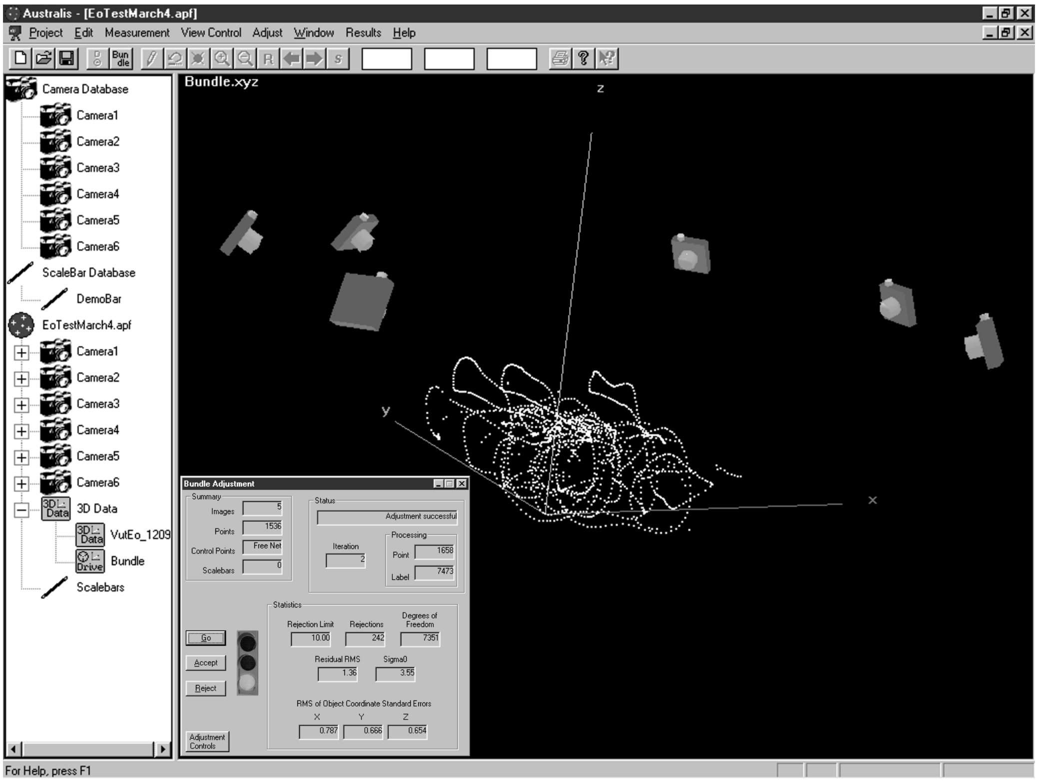

Fig. 4. Illustration of network for multi-camera, image-sequence based EO via a wand, as well as bundle adjustment dialog box.

on a Pentium PC with a 120 MHz processor using forward fold-in of the normal equations, whereas reverse fold-in for one iteration of the same network takes only 32 seconds. A further benefit of reverse fold-in is that it offers a normal equation structure, which is much more conducive to the imposition of geometric constraints between object points. These usually come in the form of redundant point-to-point distance information. Such constraints can provide the basis for multi-camera image-sequence based sensor calibration and EO as is the case of building an object point-field through the use of a targeted wand (Maas, 1998; Cerveri et al., 1998). Fig. 4 illustrates the photogrammetric network arising from the use of a wand with three targets employed to perform an EO of a 6-camera configuration used for motion analysis in biomechanics. The object point array comprises about 1800 points, mainly as a consequence of the fact that the moving wand is recorded at video rate. A satisfactory EO is achievable with an order of magnitude less points, but since the image mensuration process is automatic, there is little cost associated with including additional data. In this case, the wand was moved in a continuous motion for 30 seconds.

Such features as described above are best hidden from the non-specialist user, who needs only a few indications that the bundle adjustment has been successful. Rather than needing to peruse the output files which detail adjustment results, it is invariably sufficient to refer only to a few one-number indicators of adjustment quality. The dialog box in Fig. 4 provides such indicators, specifically the Root Mean Square (RMS) value of image coordinate residuals, the number of rejected observations, the RMS value of coordinate standard errors and a status message stating that the adjustment was successful. In a self-calibration, the 'view camera data' option can be selected to examine the derived (updated) camera calibration parameters, and the strength of the calibration can be gauged through a comparison of the variances arising from a Limiting Error Propagation versus those from the Total Error Propagation (e.g. Fraser, 1996).

Once the bundle adjustment (or spatial intersection) has been successfully processed, the network can be graphically displayed, which is a valuable visual aid. The integration of the graphics display with the bundle adjustment is also useful from an educational point of view. Since the images forming the network can be selectively enabled or disabled, it is a simple matter to examine the impact on network precision and self-calibration of interactively changing the number of camera stations and therefore the network geometry.

If there is a drawback to the automatic adoption of free-network adjustment, it is that there is a certain arbitrariness about the final origin and orientation (and possibly scale) of the XYZ object point reference coordinate system. It is therefore often necessary, though not for sensor self-calibration, to transform the object point coordinates resulting from a bundle adjustment into a given datum, generally via 3D similarity transformation. This option is also integrated into *Australis*, with a closed-form solution being employed to obtain preliminary values for the transformation parameters, thus again avoiding the need for an operator to enter such 'starting' values.

Whereas in a self-calibration adjustment, sensor calibration parameters might be viewed as a final outcome, albeit for the particular project at hand, triangulated XYZ object point coordinates invariably represent an intermediate result. Functions of these coordinates are typically of greater interest, for example parameters of shape, size, orientation, or change in shape or position in a multi-epoch survey. Thus, in a final processing step associated with photogrammetric data reduction, analysis tools are required to extract the spatial information of interest from the object space coordinates. Within *Australis*, such tools have been limited to a representative sample, mainly for educational purposes. Functions such as a best-fitting circle or plane can be applied to sub-sets of points highlighted in the Graphics View, as illustrated in Fig. 3. A further common post-processing tool is the use of the 3D similarity transformation for deformation analysis, as illustrated in Fig. 5 which shows the object point displacements resulting from the imposition of static loads on a trainer aircraft. These results were obtained in multi-epoch photogrammetric surveys involving over 100 images and 400 targets.

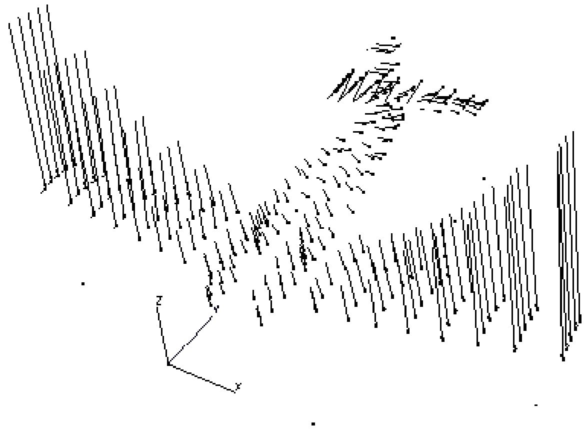

Fig. 5. Photogrammetrically measured point displacements of airplane body resulting from imposition of simulated in-flight loading; the maximum deflection at the wing tips is close to 10cm.

3. Practical considerations

A photogrammetric survey such as that of the trainer aircraft remains a relatively complex operation, requiring about two hours per epoch to record the 100-image network and perform the image mensuration and bundle adjustment. The operation, although arguably user-friendly and highly automated, nevertheless requires a good deal of photogrammetric insight and experience. On the other hand, a straightforward single-sensor survey with the prime purpose of providing a camera self-calibration needs no such experience and, so long as a few simple guidelines are adhered to, hardly constitutes an art.

To illustrate this, we give the example of the self-calibration of a Kodak DC 210 'amateur' digital camera, using *Australis*, where the process proceeds as follows:

1) A series of, say, 50 targets is placed on a wall covering the field of view of the camera, an area of about 2m x 2m being suitable in the case of the DC210. This array need only remain stable for as long as it takes to record the images and no preliminary XYZ positional data is required.

2) An EO device is placed within the target field such that it is imaged from all camera station positions.

3) A convergent network of 6-10 images incorporating orthogonal roll angle diversity is then recorded from a set-back distance of 3-4m (effectively infinity focus on the DC 210 which is zoomed to either its shortest or to its longest principal distance setting).

4) The images are imported into *Australis*, and the initial camera data comprising approximate focal length, array dimensions and pixel size are entered. (Recall that it is not imperative that the pixel size be exactly known).

5) All images are then measured as outlined above, in what is a highly automated procedure consuming about 2 minutes. No inputting of additional information or starting values by the operator is required.

6) Finally the self-calibrating bundle adjustment is run for the default camera parameter set. Depending on the anticipated use of this calibration information (e.g. medium or low accuracy),

the operator may choose to re-run the self-calibration with reduced sets of additional parameters and evaluate the impact on final precision and accuracy.

This whole process takes only about 5-10 minutes from image recording to final results, and constitutes a user-friendly operation well suited to non-specialist application. A further practical example is given by the network indicated in Fig. 3, where 200 points on a car door are measured via *Australis* with a DCS 420 camera, the complete process again consuming about 10 minutes. Such automated operations are by no means unique to *Australis* and it is noteworthy that high-end, off-line vision metrology systems employing intelligent cameras, such as V-STARS (Ganci and Handley, 1998) exhibit performance which well exceeds that just indicated.

A purpose of this paper has been to illustrate that rather than always constituting an ‘art’ (e.g. Foerstner and Guelch, 1999), camera orientation and sensor calibration can be a very fast, highly automated and straightforward process, so long as the problem domain is well bounded. There is of course a quantum leap between what is achievable by non-specialist users of *Australis* and what is sought after in the realm of generating complete 3D object descriptions from general geometric and semantic knowledge about the scene. The computation process described in this paper, which is that embedded in *Australis*, offers a complete solution in the former case, whereas in the latter case it provides only a necessary interim step to achieving the desired outcome.

4. Concluding remarks

In describing the *Australis* software system for off-line digital close-range photogrammetry, the authors have aimed to demonstrate that with appropriate computational models and processes, and with some modest operational requirements (e.g. EO devices), automated operations, like single- or multi-sensor, multi-station orientation/triangulation, calibration and point-based 3D object measurement are not only feasible, but entirely achievable in a practical manner by non-specialist users of close-range photogrammetry. Moreover, a PC-based interactive processing system exemplified by *Australis*, which has been developed primarily for use as an interactive educational tool, can greatly assist in the worthwhile endeavour of demystifying photogrammetric orientation and calibration processes, thus rendering them more suitable for broader applications in associated fields such as computer vision.

References

Ariyawansa, D.D.A.P., Clarke, T.A., 1997. High speed correspondence for object recognition and tracking. Videometrics V, San Diego, USA, 30-31 July, Proc. SPIE 3174, 70-79.

Beyer, H.A., 1995. Quality control in industry with digital photogrammetry. In: Optical 3-D Measurement Techniques III, Gruen/Kahmen (Eds.), Wichmann Verlag, Heidelberg, pp. 29-38.

Brown, D.C., 1976. The bundle adjustment – progress and prospects. Invited paper, Commission III, Proc. of XIIIth ISP Congress, Helsinki, Finland. International Archives of Photogrammetry 21(3), 33 p.

Brown, J.D., Dold, J., 1995. V-STARS – A system for digital industrial photogrammetry. In: Optical 3-D Measurement Techniques III, Gruen/Kahmen (Eds.), Wichmann Verlag, Heidelberg, pp. 12-21.

Cerveri, P., Borghese, N.A., Pedotti, A., 1998. Complete calibration of a stereo photogrammetric system through control points of unknown coordinates. Journal of Biomechanics 31(10), 935-940.

Edmundson, K.L., Fraser, C.S., 1998. A practical evaluation of sequential estimation for vision metrology. ISPRS Journal of Photogrammetry and Remote Sensing 53(5), 272-285.

Eos Systems Inc., 2000. PhotoModeler: photogrammetry measurement and 3D modeling software. http://www.photomodeler.com, accessed March 12, 2000.

Foerstner, W., Guelch, E., 1999. Automatic orientation and recognition in highly structured scenes. ISPRS Journal of Photogrammetry and Remote Sensing 54(1), 23-34.

Fraser, C.S., 1996. Network design. In: Close Range Photogrammetry and Machine Vision, K.B.Atkinson (Ed.), Whittles, Scotland, pp. 256-282.

Fraser, C.S., 1997. Digital camera self-calibration. ISPRS Journal of Photogrammetry and Remote Sensing 52(4), 149-159.

Fraser, C.S., 1998. Some thoughts on the emergence of digital close-range photogrammetry. Photogrammetric Record 16(91), 37-50.

Fraser, C.S., Shao, J., 1997. An image mensuration strategy for automated vision metrology. In: Optical 3D Measurement Techniques IV, Gruen/Kahmen (Eds.), Wichmann Verlag, Heidelberg, pp. 187-197.

Furnee, E.H., Jobbagy, A., Sabel, J.C., van Veenendaal, H., Martin, F., Andriessen, D., 1997. Marker-referred movement measurement with grey-scale coordinate extraction for high-resolution real-time 3D at 100Hz. Proc. SPIE 3173, 357-369.

Ganci, G., Handley, H.B., 1998. Automation in videogrammetry. International Archives of Photogrammetry and Remote Sensing 32 (5): 53-58.

Maas, H.-G., 1992. Complexity analysis for determination of image correspondences in dense spatial target fields. International Archives of Photogrammetry and Remote Sensing 29(B5), 102-107.

Maas, H.-G., 1998. Image sequence based automatic multi-camera system calibration techniques. International Archives of Photogrammetry and Remote Sensing 32 (5), 763-768.

Mason, S., 1994. Expert system based design of photogrammetric networks. Ph.D. dissertation Institute of Geodesy and Photogrammetry, ETH Zurich, Mitteilungen No. 53, 187 p.

ShapeQuest Inc., 2000. ShapeCapture Version 2.1 – The most advanced tool for 3D measurement & modelling from images. http://www.shapequest.com, accessed March 12, 2000.